

# Rapid sensitivity changes on flickering backgrounds: tests of models of light adaptation

Shuang Wu, Stephen A. Burns, and Ann E. Elsner

*Schepens Eye Research Institute, 20 Staniford Street, Boston, Massachusetts 02114*

Rhea T. Eskew, Jr.

*Department of Psychology-125 NI, Northeastern University, 360 Huntington Avenue, Boston, Massachusetts 02115*

Jichang He

*Schepens Eye Research Institute, 20 Staniford Street, Boston, Massachusetts 02114*

Received September 30, 1996; revised manuscript received January 27, 1997; accepted January 30, 1997

To investigate mechanisms underlying sensitivity changes that are capable of following rapid variations in intensity of the background field, we measured the threshold radiance needed to detect a 2-ms probe flash presented at various phases relative to a sinusoidally flickering background. The temporal frequency, mean luminance, and modulation of the background were systematically varied. The sensitivity change consisted of two components: a phase-insensitive increase in threshold that occurs at all the phases of the background field (a change in the dc level of the threshold), and a phase-dependent variation in threshold. Both components can reliably be measured at temporal frequencies up to approximately 50 Hz. On a 30-Hz background, the threshold varied with phase over roughly 0.5 log unit within a half-cycle (17 ms). For background flicker rates of 20–40 Hz the probe threshold increased with increasing instantaneous background radiance, following a typical threshold-versus-radiance template, and approaching Weber-law behavior during the peak of the background flicker. This pattern of threshold elevation was measured at mean background illuminances from 580 to 9100 Td (trolands), with the dimmer backgrounds being slightly less effective in producing threshold elevations. The measured increase in the dc level commenced as soon as the modulation of the background flicker began, and the amount of threshold elevation followed the envelope of the background flicker, ruling out modulation gain control explanations for the change in sensitivity on flickering backgrounds. The threshold elevations measured on a 30-Hz, 25% modulation background were lower than those measured on a 30-Hz, 100% modulation background at all phases. The measured changes in threshold with changes in background modulation rule out all adaptation models consisting of a multiplicative and a subtractive adaptation processes followed by a single, late, static nonlinearity. © 1997 Optical Society of America [S0740-3232(97)00409-2]

*Key words:* light adaptation, flicker, visual sensitivity, modulation, gain control, visual models.

## 1. INTRODUCTION

Adaptation to changes in ambient illumination is a critical function of the visual system.<sup>1,2</sup> Light levels can vary over an almost 10<sup>11</sup> range, and variations can occur rapidly. The adaptation mechanisms that the visual system has adopted include photochemical (bleaching), mechanical (pupillary changes), and neural processes (the duplex nature of the retina and neural adaptation). In this paper we probe the neural adaptation of the cone system to changes in retinal illuminance. Neural adaptation involves two types of changes in sensitivity: a decrease in sensitivity with increasing illuminance, and a speeding up of the visual response with increasing retinal illuminance. These two aspects of adaptation have led to two separate and conceptually very different approaches to both measuring and modeling the adaptation process.<sup>3</sup> The change in time scale has typically been determined by measurement of flicker modulation thresholds at different retinal illuminances. The results are then modeled with a systems model that typically includes mul-

tipole stages of light-dependent temporal filtering. Models of this type can successfully account for flicker thresholds.<sup>4–10</sup> The change in sensitivity with changes in retinal illuminance has often been measured with a probe-flash design,<sup>11–13</sup> whereby the sensitivity of the visual system to a test stimulus (the probe) is measured during rapid changes of background illuminance (the flash). Results from the probe-flash studies are typically modeled with a system including multiple stages of subtractive and multiplicative adaptation and a single, late, static nonlinearity. We refer to these multiplicative, subtractive, and nonlinear models as MUSNOL models, following Graham and Hood.<sup>3</sup> Models of this type can successfully account for the nonlinear changes in visual sensitivity associated with rapid changes in background retinal illuminance<sup>11–16</sup> but do less well at accounting for the sensitivity to rapidly changing stimuli.<sup>17,18</sup> This disparity in the domains over which the two types of models are successful has led Hood, Graham and their co-workers to propose merged models,<sup>3,18,19</sup> and these

merged models are somewhat more successful at accounting for results obtained by both approaches.

One can combine features of these two conceptual approaches to studying adaptation by measuring the change in visual sensitivity during flicker. For instance, Boynton *et al.*<sup>20</sup> measured the threshold for seeing small test flashes superimposed on flickering backgrounds. They found that test thresholds varied with background radiance up to a temporal frequency of at least 30 Hz, even for low-luminance conditions in which the 30-Hz flicker itself was imperceptible. This result suggests that adaptation may be quite rapid, a possibility in agreement with the finding of Hayhoe *et al.*<sup>13</sup> that multiplicative adaptation is complete within 50 ms. In addition, other studies that use a similar approach<sup>17,18,21–23</sup> support the possibility that light adaptation is both rapid and highly nonlinear, a possibility that cannot readily be explained by current models, including the merged models.<sup>18</sup>

Most of these models are inconsistent with the highly dynamic nonlinear adaptation that we have measured by using the electroretinogram (ERG).<sup>24</sup> The ERG results suggest that there is a modulation-dependent, rapid gain change controlling visual sensitivity. We found that the ERG data show evidence of a compressive response at 16 Hz, an expansive response near 40–48 Hz, and an approximately linear response at 56 Hz or higher frequencies. The relation between the phase of the ERG response and the stimulus modulation also varies with temporal frequency. Similar results have been obtained from the Y ganglion cells in the cat retina by Shapley and Victor<sup>25</sup> and were explained by a temporal contrast gain control: a mechanism that adjusts the gain of the retina depending on the temporal contrast rather than on the mean luminance. In addition, our ERG results had complex temporal-frequency interactions, which suggests that the gain control is both highly nonlinear and dynamic. Thus models of light adaptation may require incorporation of a dynamic nonlinear process.

The last stage of the current models based on the probe-flash paradigm is a single, static nonlinearity, as mentioned above. Thus, according to these models, dynamic changes in adaptation occur prior to the static nonlinearity. To account for these dynamic changes, the temporal properties of each stage prior to the nonlinearity must be specified. In this study we investigate these temporal properties of visual adaptation by measuring test thresholds on flickering backgrounds that systematically varied in temporal frequency, mean luminance, and modulation. The mean luminance used in our main experiment was higher than the mean luminances used by Robson and Powers<sup>17</sup> and by Hood *et al.*<sup>18</sup> We varied the frequency of the flickering backgrounds between 20 and 70 Hz in an attempt to separate subtractive and multiplicative stages based on their temporal characteristics. The data presented below (see Section 3) are organized into four experiments. In the first experiment we determined the speed of the sensitivity changes that occurred in the presence of flicker by measuring the change in sensitivity to brief test flashes with changes in the phase relation between the test flash and the flickering background. We characterized the changes in sensitivity over a range of temporal frequencies. In the second experi-

ment we tested whether the effect of the flickering background changed as a function of retinal illuminance. In the third experiment, by measuring the time course of the loss in sensitivity, we tested whether modulation gain control mechanisms could account for the loss of sensitivity during background flicker. In the final experiment we tested general predictions of all MUSNOL models by measuring the relation between test sensitivity and the modulation of the background flicker.

## 2. METHODS

### A. Subjects

Complete data sets were obtained from two subjects: One (SW) has normal vision, and the other (JH) has deuteranomalous color vision, but with good discrimination in a color-matching task. Confirmatory data points were also obtained from a third subject with normal color vision.

### B. Apparatus

A two-channel Maxwellian-view optical system, modified from a system described previously,<sup>26,27</sup> was used to deliver the stimuli. Both channels used a 594-nm He-Ne laser as the light source. Each laser beam was passed through a rotating holographic diffuser (Physical Optics Corp.) to eliminate speckle. In one channel we presented a flickering background; in the other we presented a circular test target. The edges of the two fields were optically conjugate and were in good focus for both observers. The two channels were then combined with a beam splitter, so that the subject saw the test stimulus superimposed on the background field. Neutral-density filters were used to control the average retinal illuminance of each channel, and a common neutral-density wedge was used to vary the overall retinal illuminance. During testing, we chose a dust speck near the center of the background field to serve as a fixation target.

The temporal modulation of both channels was controlled by a programmable function generator (Qua-Tech, Inc.) with a 12-bit digital-analog converter and a multiplier. The output of the multiplier was converted by a voltage-controlled oscillator to a pulse frequency, which then drove the acousto-optic modulator through pulse density modulation.<sup>28</sup> Each pulse was 2  $\mu$ s in duration. For the background, the average pulse frequency was approximately 100 kHz. The final light output was linearly related to the input, up to the resolution of the photodetector used for calibration purposes.

### C. General Stimuli: Background Flicker

The background field was circular and 9.5 deg in diameter. An example of the temporal profile of a 30-Hz flickering background is shown in Fig. 1. This background consists of a Gaussian-windowed sine-wave flicker, which has the following form:

$$G(t) = I_{\text{mean}}\{1 + \exp[-(2\pi ft/\sigma_f)^2]\sin(2\pi ft)\},$$

where  $G(t)$  represents the instantaneous radiance of the background as a function of time  $t$ ,  $I_{\text{mean}}$  represents the mean luminance of the background [2300 trolands (Td)],  $f$  denotes the temporal frequency of the flicker, and  $\sigma_f$  con-

trols the width of the Gaussian envelope. When the temporal frequency was varied, the width of the Gaussian envelope was adjusted inversely to keep a constant  $\sigma_f$  ( $=20$  cycles), thus providing constant stimulus power.<sup>29</sup> The Gaussian-windowed stimulus was chosen to avoid long-term flicker adaptation and transient effects due to abrupt flicker onset.<sup>30</sup>

#### D. Test and Control Conditions

The test stimulus was a 2-ms, 1.6-deg-diameter, circular test flash with a sharp spatial edge. It was superimposed in the center of the background field. The phase relation between the test flash and the background stimulus was under program control. In most experiments the phase of the test flash was varied across the central cycle of the background flicker in nine 45-deg steps from  $-180$  to  $180$  deg.<sup>31</sup> In addition to the test conditions we incorporated a control condition into every experimental session. The control condition was identical to the test conditions, except that the test flash was presented prior to the onset of background flicker, at  $-3600$  deg (Fig. 1, top).

#### E. Stimuli for Individual Experiments

##### 1. Experiment 1: Variation of Temporal Frequency

Test thresholds were measured on background frequencies of 20, 30, 40, 50, 60, and 70 Hz. The modulation of

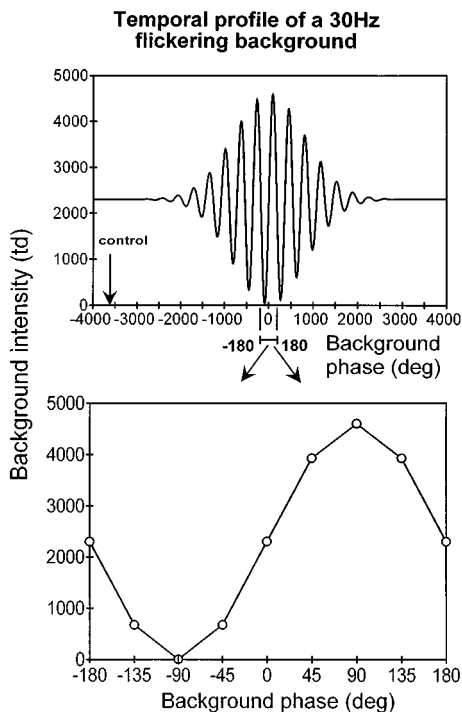


Fig. 1. Top: temporal profile of the Gaussian-windowed flickering background at 30 Hz used in this study. The modulation of the background radiance as a function of time is given by  $G(t) = I_{\text{mean}}\{1 + \exp[-(2\pi ft/\sigma_f)^2]\sin(2\pi ft)\}$ , where the mean luminance of the background ( $I_{\text{mean}}$ ) was 2300 trolands (Td) and  $\sigma_f$  was 20 cycles (corresponding to  $\sigma_t = 75$  ms). The downward-pointing arrow on the left indicates a control condition in which the test stimulus was presented at a background phase of  $-3600$  deg (10 cycles preceding the maximum flicker). This threshold measured in this control condition provided a measure of the threshold sensitivity of the visual system at the mean luminance. Bottom: modulation of the background radiance within the central cycle. The open circles indicate the background phases at which the test stimuli were presented.

the background within the central cycle was 100%, with a mean retinal illuminance of 2300 Td. The test flash was presented at temporal phases from  $-180$  to  $180$  deg, in 45-deg steps.

##### 2. Experiment 2: Variation of Mean Retinal Illuminance

Test thresholds were measured on 30- and 50-Hz backgrounds at mean retinal illuminances of 580 and 1150 Td, as well as at 2300 Td from experiment 1. In addition, one subject (SW) was also tested at 9100 Td. Background modulation was 100%.

##### 3. Experiment 3: Variation of Threshold within the Flicker Envelope

Test thresholds were measured at background phases of  $-3600$ ,  $-1800$ ,  $-1440$ ,  $-1080$ ,  $-720$ ,  $-360$ ,  $0$ ,  $360$ ,  $720$ ,  $1080$ ,  $1440$ ,  $1800$ , and  $3600$  deg. These phases were all multiples of 360 deg, thus corresponding to the zero-crossing points of the Gaussian-windowed stimulus, i.e., when the instantaneous background radiance was at a mean retinal illuminance of 2300 Td. The background was flickering at 30 Hz at 100% modulation.

##### 4. Experiment 4: Variation of Modulation

Test thresholds were measured for background flicker modulations of 25% and 50%, in addition to 100% from experiment 1. Background flicker frequencies were either 30 or 50 Hz. The mean retinal illuminance of the background was 2300 Td.

#### F. Psychophysical Procedure

Thresholds were determined with a two-interval, two-alternative, forced-choice paradigm. The mean luminance of the background was maintained constant at all times during the experimental session. In one interval only the background flicker was presented. In the other interval both the test flash and the background flicker were presented. Each interval was 3 s in duration. The peak of the background flicker modulation occurred at 2 s. The start of a new trial was initiated immediately after the subject indicated, by pressing one of two buttons, which interval contained the test flash. The luminance of the test was initially set at an arbitrary level (approximately 0.7 log unit below the mean luminance of the background) and was then increased after one incorrect judgment or decreased by the same amount after two consecutive correct judgments. The initial step size was 0.2 log unit and was then reduced to 0.1 log unit after the first reversal and to 0.05 log unit after the second reversal. An experimental session typically consisted of four randomly interleaved staircases (three test conditions and a control condition) at a single background frequency. Each staircase consisted of 12 reversals. The mean of the last nine reversals for each condition was taken as the estimate of the test threshold. Other than the control condition, the background phases tested within each session were randomized in sequence. To obtain data for the nine standard phase conditions for each frequency, we typically collected data from three experimental sessions at a single frequency on a single day. All the frequencies were tested once before any was repeated. Each fre-

quency was tested three to five times for each subject. Results presented are the means of the three to five threshold determinations. Experiments 1, 2, and 4 were randomly interspersed, while experiment 3 was conducted separately.

### 3. RESULTS AND DISCUSSION

#### A. Experiment 1

Test threshold varied systematically with the background phase. Figure 2 compares the thresholds obtained with a 30-Hz flickering background (top) with the intensity of the background field (bottom). For convenience, we describe the threshold change by separating it into two components: a phase-dependent variation in threshold, and an overall increase in threshold in the presence of flicker. The first component is represented by the peak-to-trough threshold difference. For the 30-Hz background flicker, threshold is minimum at a background phase of  $-90$  deg (dimmiest background intensity) and increases by approximately 0.5 log unit when measured at a background phase of  $90$  deg (brightest background intensity). However, this threshold variation is not sinusoidal. The second component of the threshold change is represented by the elevation of the mean threshold relative to the sensitivity measured prior to the onset of background flicker (at  $-3600$  deg; see Fig. 1). This change in average sensitivity also has a magnitude of approximately 0.5 log unit at 30 Hz. We refer to this component of the threshold elevation as the dc level.<sup>18</sup> Both the change in dc level and the phase-dependent changes in sensitivity were far greater than the session-to-session variability in setting the thresholds. At 30 Hz the total threshold change for the two conditions was approximately 1 log unit, whereas the standard deviation of the control thresholds at 30 Hz was 0.12 and 0.08 log unit for observers SW and JH, respectively.

The increase in threshold depended on both the frequency and the phase of the background flicker (Fig. 3). With increasing background frequency, both the phase-dependent threshold variation and the dc level decrease. We were able to measure threshold elevations reliably to approximately 50 Hz. The phase at which the maximum threshold elevation occurred also increased with increasing frequency from 20 to 40 Hz. At 50 Hz, although there was a reliable phase-dependent increase in threshold, it was small in amplitude and differed somewhat between observers.

The thresholds measured in the control conditions do not depend on either the background frequency or the modulation of the background (see experiment 4) for stimuli at 30 Hz and higher. This supports the assumption that, when presented on a steady field of the same time-average retinal illuminance, the control conditions represent an adequate estimate of the sensitivity of the visual system to the test flash. However, for the 20-Hz background conditions the control condition thresholds were consistently elevated relative to all the other frequencies [ $t(19) = 9.82$ , and 3.85 for SW and JH, respectively;  $p < 0.01$ ]. This could be because the 20-Hz background is farther above its own flicker threshold than are

the other backgrounds and produces a generalized loss in sensitivity. We did not include the 20-Hz control condition in other analyses.

#### B. Discussion: Effect of Temporal Frequency

The frequencies that we used in the current experiments extend well beyond those used in previous studies. Nevertheless, as in the previous studies, the measured change in the dc level is a robust and consistent feature of the threshold elevation.<sup>18,20,21</sup> The phase-dependent threshold variation that we measured at high frequencies is both large and rapid. For example, on the 30-Hz background, a 0.5-log-unit variation in threshold (Fig. 2) occurs within 17 ms (i.e., half-period of 30 Hz).<sup>32</sup>

To better show the relation between the measured test threshold and the intensity of the background field at the

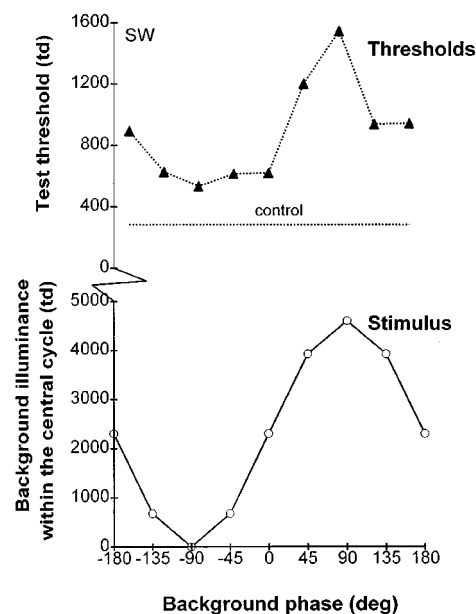


Fig. 2. Top: test thresholds measured on a 30-Hz flickering background as a function of the background phase. Subject, SW. The horizontal line labeled "control" shows the average threshold measured in the control condition. Bottom: same as the lower panel of Fig. 1.

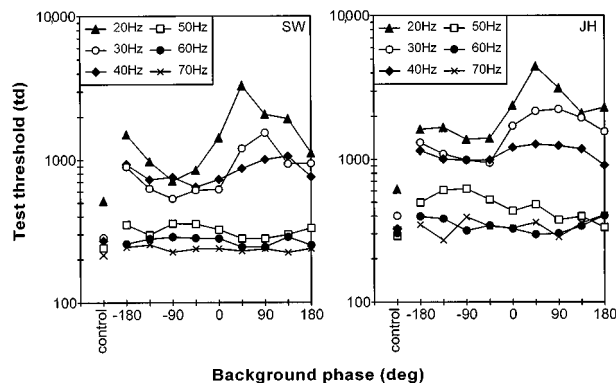


Fig. 3. Test thresholds as a function of the background phase for all temporal frequencies. The data points plotted in the left-most columns are the average thresholds measured in the control conditions (see labels at bottom left of each plot). The retinal illuminance was 2300 Td.

time of the test flash, we replotted the data of Fig. 3 as threshold-versus-radiance (tvr) curves, where the background radiance is the instantaneous radiance of the background. However, since in some of the results there was a phase shift between the variation in threshold and the variation in the illuminance of the background, we first corrected for this phase shift. Figure 4 illustrates the procedure used to correct for the phase shift.

In Fig. 4(a), log test thresholds for a 20-Hz background (from subject SW) were plotted as a function of the background phase. Two features of the data are worthy of note. First, the threshold variation appeared more sinusoidal in shape when plotted as log thresholds than when plotted on a linear scale; and, second, the maximum threshold elevation did not occur at the maximum of the background flicker (unlike the 30-Hz data shown in Fig. 2). In Fig. 4(b) we replotted the thresholds plotted in Fig. 4(a) as a function of the background radiance at the time the test flash is presented rather than as a function of the background phase. A systematic pattern can be seen in this plot: At the same instantaneous background radiance (for example, data points 1, 5, and 9), the threshold measured earlier in time was consistently higher than that measured later in time. This result is due, at least in part, to the phase shift mentioned above. In Fig. 4(c), we corrected for the phase shift between the threshold and the background variations by fitting the 20-Hz threshold measurements (filled circles) with a sine wave (solid curve) that was constrained to have a temporal frequency of 20 Hz but which varied in amplitude and phase. From the best-fitting sine wave we then computed the equivalent instantaneous illuminance of the background for each test flash. We performed this phase correction at each frequency, restricting the sine wave to the frequency of the background flicker for that condition. In Fig. 4(d) the test thresholds were then replotted as a function of the phase-adjusted background radiance. With this phase adjustment the test threshold increased monotonically with increasing phase-adjusted background radiance.<sup>33</sup> The numbers next to each data point, identifying the temporal sequence of the thresholds, now lie interspersed.

This analysis of the thresholds based on the phase-adjusted background intensity allows us to compare the thresholds measured on flickering backgrounds with the threshold that would be measured if the background illuminance had been maintained at that particular intensity long enough for threshold to reach a steady-state value (we shall call this complete adaptation). However, the distortion present in the log threshold relation suggests that the factors controlling sensitivity are more complex than are captured by this simple analysis.

The phase-adjusted test thresholds for all the frequencies are shown as data points in Fig. 5. The solid curves represent the moving averages of the individual data points. The moving average was calculated as the mean of three adjacent phase-adjusted threshold determinations. The 20-Hz thresholds now increase with increasing background illuminance similar to a standard tvr function, approaching Weber-law behavior at the highest background intensities; within the 95% confidence interval, the slope of the last five data points is  $1.01 \pm 0.24$  for

SW and  $0.80 \pm 0.23$  for JH. This suggests that, at these high instantaneous background illuminances, adaptation mechanisms are still following the rapid changes in background in much the same way that they would to much slower changes in retinal illuminance. That is, the data for the brightest portions of the background flicker follow Weber's law. At 70 Hz, the tvr curve is essentially flat, showing no evidence of adaptation to the instantaneous background illuminance. Data from other frequencies lie between 20 and 70 Hz, with an abrupt loss in background effectiveness occurring between 40 and 50 Hz and with background flicker rates higher than 50 Hz having no reliable effect on the measured thresholds.

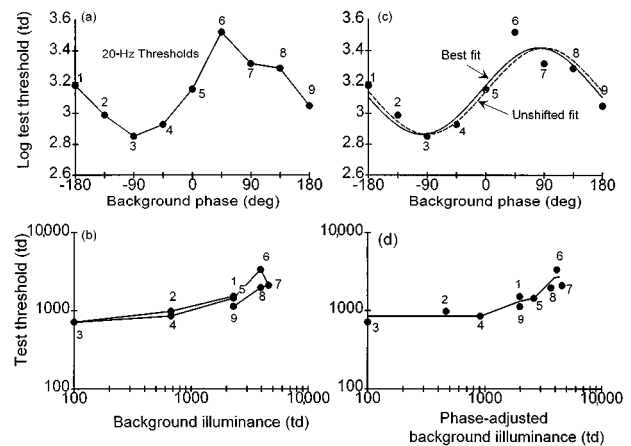


Fig. 4. Illustration of the phase-adjustment procedure. (a) Log test thresholds measured on a 20-Hz flickering background as a function of the background phase. Subject, SW. (b) The same thresholds as a function of the instantaneous background radiance. The number next to each data point indicates the temporal sequence in which it was measured. (c) Same as (a), but with the best-fitting sine wave (solid curve) superimposed on the data points. The dashed curve shows an unshifted version (relative to the stimulus phase) of the same sine wave. The phase shift between the two curves was then used to compute the phase-adjusted background radiance. (d) Same as (b), but the thresholds are now plotted against phase-adjusted background radiance.

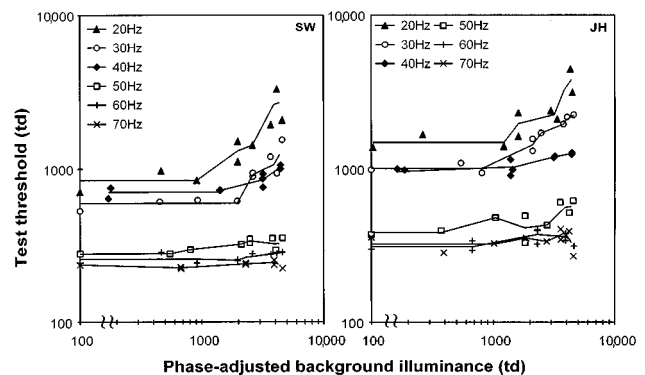


Fig. 5. Test thresholds as a function of the phase-adjusted background radiance for all the temporal frequencies. The curves drawn among the data points are the moving averages (over 2–3 data points). The phase adjustments applied to data at 20, 30, 40, and 50 Hz are 7.9,  $-8.4$ ,  $-22.7$ , and  $184.5$  deg, respectively, for subject SW and  $17.2$ ,  $4.7$ ,  $23.3$ , and  $168.1$  deg for subject JH.

### C. Experiment 2

Data obtained at all mean luminances for temporal frequencies of 30 and 50 Hz are shown in Fig. 6. The relation between test threshold and phase-adjusted radiance is presented in Fig. 7. Thresholds measured in the control conditions (Fig. 7, thick solid curves) follow Weber's law, with a slope close to 1. The 30-Hz data (Fig. 6, left) show the same two components of threshold elevation as discussed above, with the first component being the variation in threshold as a function of the phase-adjusted instantaneous background radiance and the second component being the change in the dc level relative to the control condition. The threshold variation is evident at the highest background radiances, where the slopes of the tvr curves approach 1 asymptotically (Fig. 7). This Weber's law asymptote suggests that the gain control mechanisms are following the background flicker and are producing Weber-like behavior, but with an overall loss of sensitivity relative to the control measurements.

The 50-Hz data (Fig. 6, right) show the threshold elevation expected for the mean luminance; that is, they fall near the threshold for the control condition. However, they also show a small, but consistent, increase in the dc level. This increase in the average threshold is especially evident at higher mean luminances. However, the thresholds have only a minimal phase-dependent change in sensitivity, and the resulting tvr curves are relatively flat (Fig. 7, right).

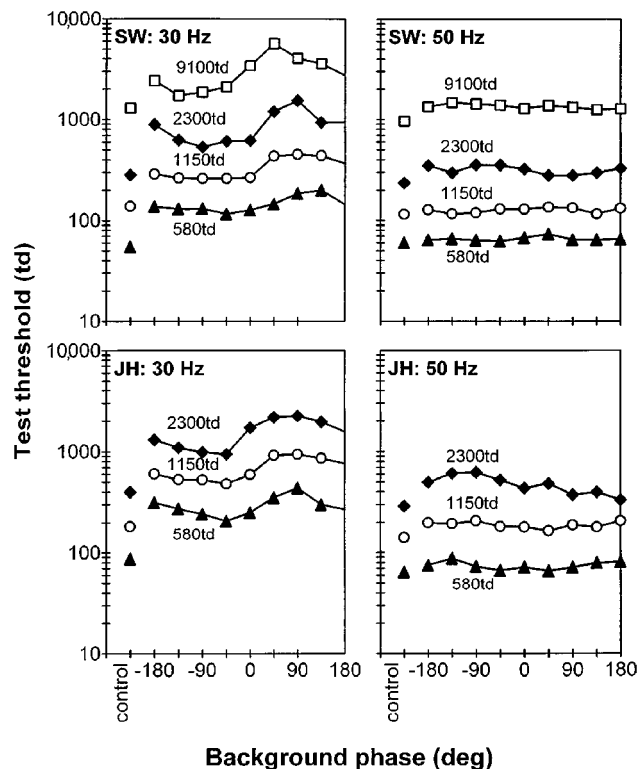


Fig. 6. Test thresholds as a function of the background phase at different mean illuminances. Data are shown for 30 Hz (left) and 50 Hz (right) for both subjects. The data points plotted in the leftmost columns are the average thresholds measured in the control conditions.

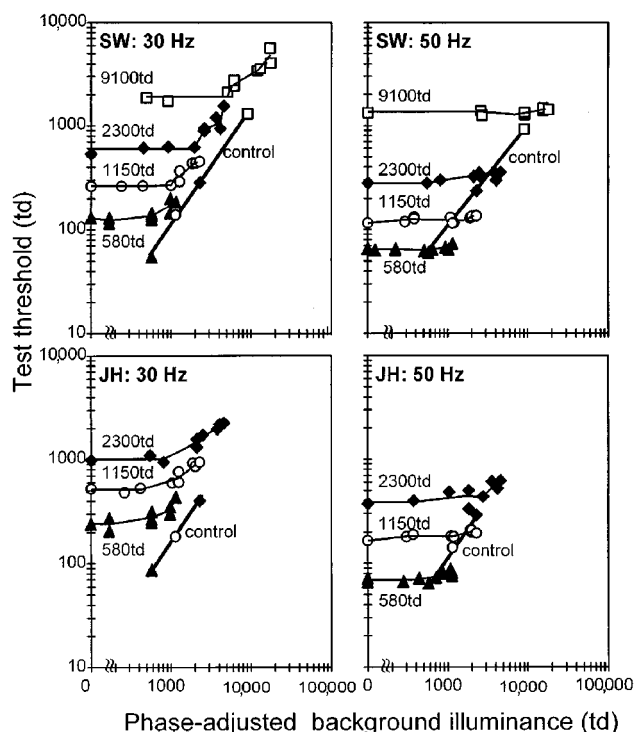


Fig. 7. Same data as in Fig. 6, but plotted as a function of the phase-adjusted background radiance. The data points connected by the heavy solid curves are the thresholds measured in the control condition, which increase with increasing mean illuminance according to Weber's law. The phase adjustments for SW's data at the four mean illuminances, respectively, are  $-0.01$ ,  $-7.2$ ,  $-8.4$ , and  $18.9$  deg at 30 Hz and  $38.0$ ,  $41.8$ ,  $184.5$ , and  $180.4$  deg at 50 Hz. For JH, the phase adjustments at the three mean illuminances, respectively, are  $0.03$ ,  $-5.4$ , and  $4.7$  deg at 30 Hz and  $256.0$ ,  $227.2$ , and  $168.1$  deg at 50 Hz.

### D. Discussion: Experiment 2

The results from the mean luminance experiment show that, for the 30-Hz background stimulus, the visual system is able to rapidly adjust its sensitivity to the instantaneous background radiance at all the retinal illuminances tested, but the fast component of adaptation did not look simply like a low-pass-filtered version of the steady-state adaptation behavior of the system. To visualize what one could expect if adaptation mechanisms responded only to a temporally filtered transformation of the background illuminance, we can consider two possible types of visual adaptation, schematically shown in Fig. 8.

First, consider a hypothetical system that instantaneously adapts to the background radiance and obeys Weber's law. For this system, threshold would increase in proportion to the background radiance, producing tvr curves that fall on a curve with a slope of 1, as illustrated by the hypothetical tvr curve labeled "fast." The only limiting factor for this hypothetical curve is the amount of dark light or noise, which comes into play at the low background intensities. Such a system would produce a classic tvr curve even for flickering backgrounds, and the shape of all the threshold-versus-phase plots shown in Fig. 6 would be sinusoidal. This hypothetical visual system can be thought of as obeying Weber's law at each point in time. Next, consider an alternative, hypothetical system that adapts very slowly and is entirely insen-

sitive to rapid background modulations. The adaptation state of this latter system would be constant across background phase, and sensitivity would be determined entirely by the mean luminance of the background. This is illustrated by the dotted line in Fig. 8. Simple temporal filtering would cause the measured threshold to lie somewhere between these extremes, depending on the flicker frequency and the amount of filtering. A prediction for such a low-pass adaptation mechanism is shown by the heavy curve labeled “intermediate” in Fig. 8. However, the actual 30-Hz data (filled circles) do not follow either of these hypothetical extremes; nor do they lie in between. They are elevated, a change that we describe as a shift in the dc level. In addition, the increase in threshold with increasing retinal illuminance occurs mainly at high background intensities. For these high instantaneous intensities the change in sensitivity with illuminance approaches a simple multiplicative change in sensitivity (a vertical translation of the tvr curve), whereas at low instantaneous backgrounds there is an asymptotic lower limit on the threshold. At 50 Hz the data do appear more like what is expected from a slow adaptation mechanism, with only a small change in the dc level.

The dc level is lower at 50 Hz than at 30 Hz. One possible cause of this dc level change is a simple frequency-limited gain control, some form of which is included in all models of light adaptation (we refer to this as a simple gain control hypothesis). This hypothesis requires a non-linearity asymmetric around the mean luminance after the filtering stage to produce the change in the dc level.<sup>11–13</sup> These types of model are typified by MUSNOL<sup>3</sup>-type models. A second type of mechanism is a gain control that adjusts sensitivity depending on the modulation of the stimulus during each presentation of the background. We refer to this as a modulation gain control hypothesis<sup>25</sup> to parallel the contrast gain controls hypothesized to be active in spatial vision. By definition,

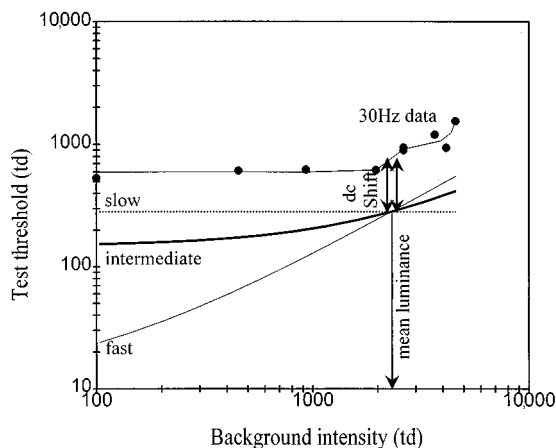


Fig. 8. Schematic diagram showing what one might expect based on two adaptation mechanisms: a mechanism that completely adapts to the background radiance at every point in time (the curve labeled “fast”), and a mechanism that is entirely determined by the mean luminance (the curve labeled “slow”). If sensitivity is determined as an intermediate between these extremes, then the data should lie in between these extremes (e.g., the heavy curve labeled “intermediate”). However, the 30-Hz test thresholds (filled circles) are elevated relative to both hypothetical cases.

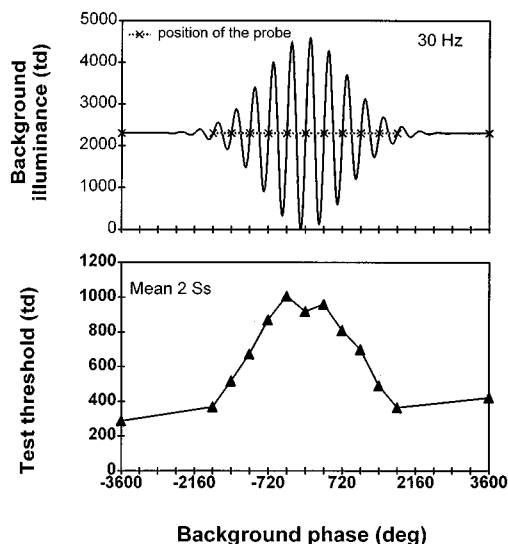


Fig. 9. Top: temporal profile of a 30-Hz flickering background with the  $\times$ 's indicating the temporal positions at which the test stimuli were presented. The background phases at each of these positions are all multiples of 360 deg, so the stimulus was presented when the background field was at the mean retinal illuminance. Bottom: mean thresholds of two subjects, measured at the background phases indicated in the upper panel.

a modulation gain control mechanism would require integration over at least one cycle of the stimulus to obtain an estimate of stimulus modulation. Thus, if a modulation gain control is active in setting thresholds in the presence of the flickering backgrounds, then the measured threshold elevation should lag behind the envelope of the background flicker. The predictions of a modulation gain control mechanism were tested in experiment 3 by measurement of the test threshold at different temporal positions within the Gaussian envelope. Predictions of MUSNOL models were tested in experiment 4.

### E. Experiment 3: Results

Test stimuli were presented at phases that are multiples of 360 deg ( $\times$ 's in Fig. 9, top), at which the instantaneous background luminance is at the mean level. Measurements were made for the 30-Hz background, since it produces minimal phase shifts. Test thresholds measured from the two subjects are similar in pattern, differing mainly in the absolute threshold elevation. The average of the two observers is shown in Fig. 9 (bottom). Threshold elevation closely followed the Gaussian envelope, with no evidence of delay in onset or in the threshold peak relative to the peak of the envelope.

### F. Experiment 3: Discussion

Since thresholds were measured at the zero-crossing points of the background stimulus, the threshold elevation is a measure of the dc level. As mentioned above, the modulation gain control hypothesis requires the mechanism to sample over a relatively long period of the stimulus, which predicts a delay of threshold elevation relative to the Gaussian envelope. However, we find that the test threshold depends on the modulation within the stimulus cycle in which the test was presented, with the threshold variation following the Gaussian envelope.

Thus the system must be able to resolve at least two temporal positions separated by one stimulus cycle at 30 Hz. The result rejects the modulation gain control hypothesis in its simple form.

#### G. Experiment 4

Test threshold measured on flickering backgrounds increases with increasing background modulation (Fig. 10). For both subjects there are reliable increases both in the phase-dependent component of the threshold variation and in the dc level. The threshold measured during the dimmer periods of the 100% modulation are higher than those measured during the dimmer periods of the 25% modulation background, even though the background illuminance for the 100% modulation stimulus (0 Td) was less than for the 25% modulation background (575 Td). In one subject (JH), the slopes of the 30-Hz tvr curves (Fig. 11, lower left) change slightly, depending on the modulation, being close to 1 at 25% modulation but shallower at higher modulations. This was not seen for SW, for whom the tvr curves appear to be translated without a change in slope. At 50 Hz (Fig. 11, right), there is still a small increase in the dc level, especially at 100% background modulation, but there is no evidence of systematic variation in test threshold with the background radiance.

#### H. Experiment 4: Discussion

As mentioned in Section 1, models based on the probe-flash paradigm generally include multiple stages of filtering, multiplicative and subtractive adaptation processes,

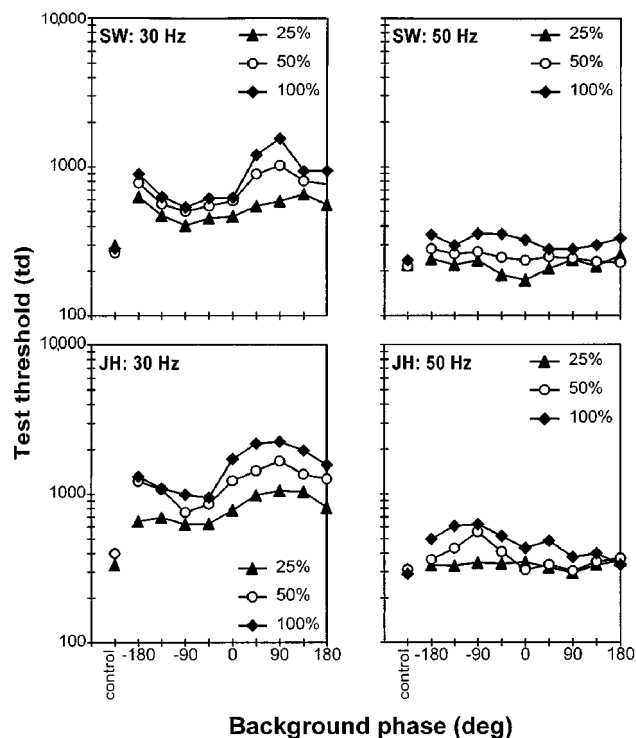


Fig. 10. Test thresholds as a function of the background phase at different modulations. Data are shown for 30 Hz (left) and 50 Hz (right) and for both subjects. The data points plotted in the leftmost columns are the thresholds measured in the control conditions, which are essentially independent of the background modulation (and are thus averaged in subsequent data analysis).

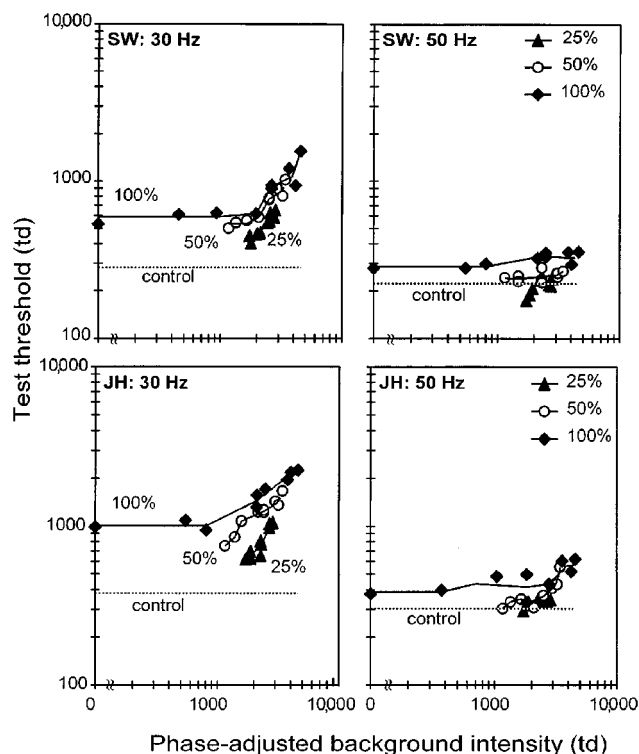


Fig. 11. Same data as in Fig. 10, but plotted as a function of the phase-adjusted background radiance. The horizontal dotted lines show the thresholds measured in the control condition, which do not vary with the background modulation. The phase adjustments for SW's data at the three modulations, respectively, are  $-29.8$ ,  $-10.9$ , and  $-8.4$  deg at 30 Hz and  $-83.5$ ,  $180.1$ , and  $184.5$  deg at 50 Hz. For JH, the phase adjustments at the three modulations, respectively, are  $1.4$ ,  $-6.6$ , and  $4.7$  deg at 30 Hz and  $180.1$ ,  $190.5$ , and  $168.1$  deg at 50 Hz.

and a single, late, static nonlinearity (see, for example, Hayhoe *et al.*<sup>13</sup>). A schematic diagram of the generic form of these MUSNOL models is shown in Fig. 12. We now consider whether this class of models can explain our results.

For simplicity, first assume that the model stages prior to the nonlinearity do not produce a modulation-dependent dc level. In such a case, at the input to the static nonlinearity, the range of values for a low-modulation stimulus constitutes a subset of the entire range covered by the 100% modulation stimulus, with both ranges of values modulating around the same mean. At the output of the static nonlinearity, the low-modulation values will still be a subset of the high-modulation values, as long as the nonlinearity itself is monotonic. Both sets of thresholds will be anchored around the same value, corresponding to the threshold obtained at the mean luminance, which is independent of the modulation. Thus all the models of this class predict overlapping tvr curves of the same slope for stimuli of different modulations, a prediction clearly inconsistent with the data given in Fig. 11.

However, in fact, the adaptation stages of a typical MUSNOL model can produce a modulation-dependent increase in the dc level [see Eq. (A2) in Appendix A]. This change in mean level can cause thresholds taken from different background modulations to fall on different points

on the static nonlinearity. In Appendix A we prove that the change in mean level with modulation is not sufficient to bring the 25% modulation thresholds outside the range of the 100% modulation thresholds, as was found in Fig. 11. This very general result requires only the following conditions: (a) The controlling pathway of the multiplicative adaptation stage must consist of constant-parameter linear filters; (b) If there is a second nonmultiplicative stage of adaptation following the multiplicative stage, it must be subtractive (i.e., not additive); and (c) The nonlinearity must be static and late. Thus our results reject this entire class of MUSNOL models with a single, late, static nonlinearity.

## 4. GENERAL DISCUSSION

### A. Modeling Considerations

As mentioned in Section 1, the stimulus paradigm<sup>20</sup> used in this study involves both a flicker modulation of the background and a brief increment of the test, thus combining two experimental approaches. It is expected that the results obtained will be predicted best by a merged model, which can predict results from each experimental approach alone. We attempted to simulate our main results (Fig. 3), using the merged model proposed by Wiegand *et al.*,<sup>19</sup> which has time-varying filter parameters and therefore is not ruled out by our data. The model, in its current form,<sup>19</sup> is clearly not fast enough, as the controlling parameters of the first low-pass stage were tailored such that they can explain the major effect of adaptation to the mean luminance. If we simply speed up these controlling parameters, the prediction at the high-frequency end showed fluctuations (owing to resonance) and failed to predict flicker modulation thresholds. Thus this approach is not feasible.

We also evaluated a general MUSNOL model by using our modulation results (see Appendix A). Such a model consists only of linear filters and multiplicative and subtractive adaptation prior to a late static nonlinearity. The filters scale the effect of modulation but cannot produce the results shown in Fig. 11. At the multiplicative stage, the multiplication of the two cosines produces a modulation-dependent dc term, a  $1f$  term, and a  $2f$  term. At the subtractive stage, as long as the  $2f$  term is not reduced relative to the dc term (i.e., as long as the subtractive stage is implemented by a high-pass filter, or at least not by a low-pass filter), then with increasing modulation the lower minima of the  $1f$  and the  $2f$  terms compensate for the increase in the dc term. (If the subtractive stage precedes the multiplicative stage, then the modulation-

dependent dc is filtered out before the multiplication, which guarantees the subset relationship.) The static nonlinearity does not alter this relationship. Based on this reasoning, in Appendix A we prove that a MUSNOL model will always predict a lower minimum threshold at 100% modulation than that at a lower modulation. Since our modulation results are inconsistent with this prediction, we can reject the entire class of MUSNOL models. Indeed, to rescue this class of models, one would need either to include an early nonlinearity in the control pathway (before the box labeled B in Fig. 12) or to replace the late, static nonlinearity with a dynamic nonlinearity.

### B. Backward Masking

Shickman<sup>21</sup> also measured the increment thresholds on sinusoidally modulated backgrounds at frequencies between 3.1 and 10 Hz. It was found that the maximum threshold elevation typically occurred before the peak background radiance (i.e., at background phases  $<90$  deg). Our data at 20 Hz also showed this tendency (Fig. 3). Shickman attributed the results to processes that produce backward masking by the modulated background. Similar conclusions were drawn by Maruyama and Takahashi.<sup>22</sup> However, Shickman did not theoretically account for the mechanisms underlying this effect other than to speculate that the ganglion cell discharge patterns seem to be correlated with the threshold measurements. While backward masking is a complicated process that involves a variety of highly nonlinear phenomena,<sup>34</sup> we are not aware of a specific masking model that is directly applicable to our data. For the two components of the threshold change measured in our data, the phase-dependent component shows a phase shift with temporal frequency and suggests an adjustment in temporal dynamics that cannot easily be explained as a masking model without further elaboration. In contrast, the change in the dc level (Figs. 2 and 3) could be interpreted as masking. However, we found that the dc threshold elevation is approximately symmetrical around the central cycle that contains the maximum flicker (Fig. 9). In addition, the elevation in the dc level approximately parallels the change in the phase-dependent portion of the threshold elevation with changes in both frequency (experiment 1) and modulation (experiment 4). These parallels argue against an explanation based on backward masking alone. In addition, a simple addition of masking noise fails to explain the approach of the steady-state tvr curves (measured in the control conditions) to the test tvr's, at high instantaneous radiances (Fig. 7). The vertical displacement of the tvr curves on

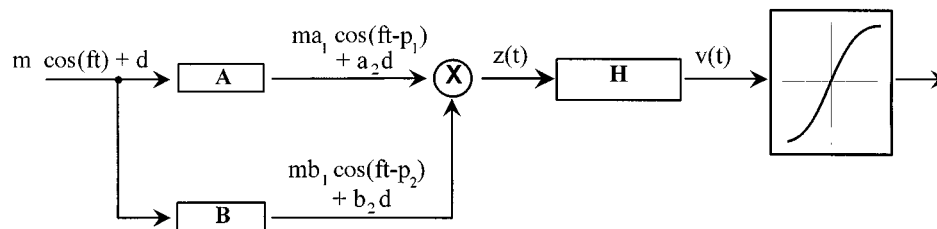


Fig. 12. Schematic drawing of a generic MUSNOL model. The multiplicative stage of the model is implemented by low-pass filters A and B, where A scales the input signal, and B controls the output of A. The signal produced by the multiplication [ $z(t)$ ] then passes through a subtractive stage, implemented by a high-pass filter H, producing a signal [ $v(t)$ ] that is fed into a static nonlinearity.

flickering backgrounds suggests a multiplicative rather than an additive effect of background modulation, ruling out a simple additive-noise component produced by the flickering background.

### C. Summary

The visual system can change its sensitivity rapidly when the retinal illuminance changes rapidly. At background temporal frequencies between 20 and 40 Hz, the threshold varied as a function of phase-adjusted background radiance following a typical tvr template and approached Weber-law behavior at high background radiances. When the mean luminance of the background was varied, the threshold measured on 30-Hz flickering backgrounds showed the expected adaptation to the mean luminance, an overall increase in the dc level owing to the presence of the flickering backgrounds, and a phase-dependent change in threshold that depended on the instantaneous background radiance. The change in the dc level during background flicker cannot be explained by a conventional modulation gain control. When the modulation of a 30-Hz background was varied, the thresholds produced by a 25% modulation background were lower than those produced by a 100% modulation background at the low background intensities. We conclude that MUSNOL models of visual adaptation cannot account for the change in visual sensitivity during rapid changes in retinal illuminance.

## APPENDIX A

The data presented in Figs. 10 and 11 show that thresholds produced with a background modulation of 25% fall below those with a 100% background modulation. Our purpose in this appendix is to demonstrate that reducing the background modulation must produce thresholds that are a subset of the range of thresholds obtained at higher background modulations for MUSNOL models containing a single, static, monotonic nonlinearity. Thus these models cannot explain the modulation data that we obtained.

The model shown in Fig. 12 contains three filters. Filter A represents the main filtering of the input signal; B represents the filtering of the signal used for multiplicative adaptation. A and B may be low-pass, bandpass, or high-pass filters (realistically, B should be slower than A, but this restriction is not necessary for the present proof). H is a high-pass filter used to model subtractive adaptation [equivalently, H could be replaced by a subtraction of a low-pass feed-forward copy of  $z(t)$ ]. The final output,  $v(t)$ , is passed through a monotonic static nonlinearity before it reaches the decision stage.

The input is sinusoidal with modulation  $m$  ( $0 \leq m \leq 1$ ), frequency  $f$ , and dc level  $d$  ( $d$  must be  $\geq 1$ ). The two filters simply rescale the input frequency by gains  $a_1$  and  $b_1$  and the dc by gains  $a_2$  and  $b_2$ , and they shift the phase by  $p_1$  and  $p_2$  (see Fig. 12).

Thus the signal after the multiplication,  $z(t)$ , is given by

$$\begin{aligned} z(t) = & m^2 a_1 b_1 \cos(ft - p_1) \cos(ft - p_2) \\ & + m a_2 b_1 d \cos(ft - p_2) + m a_1 b_2 d \cos(ft - p_1) \\ & + a_2 b_2 d^2. \end{aligned}$$

Because absolute phase is irrelevant, we may set  $p_1 = 0$  and  $p_2 = p$ . Since

$$\begin{aligned} \cos(ft) \cos(ft - p) &= (1/2)[\cos(p) + \cos(2ft - p)], \\ z(t) &= [(1/2)m^2 a_1 b_1 \cos(p)] + a_2 b_2 d^2 \\ &+ [(1/2)m^2 a_1 b_1 \cos(2ft - p)] + m a_2 b_1 d \\ &\times \cos(ft - p) + m a_1 b_2 d \cos(ft). \end{aligned}$$

The high-pass filter H has gains of  $h_0$ ,  $h_1$ , and  $h_2$  at frequencies of 0,  $f$ , and  $2f$  Hz and phase shifts of  $q_1$  and  $q_2$  at the last two of these frequencies. Thus

$$\begin{aligned} v(t) &= [(1/2)h_0(m^2 a_1 b_1) \cos(p)] + h_0 a_2 b_2 d^2 \\ &+ [(1/2)h_2(m^2 a_1 b_1) \cos(2ft - p - q_2)] \\ &+ h_1 m a_2 b_1 d \cos(ft - p - q_1) \\ &+ h_1 m a_1 b_2 d \cos(ft - q_1). \end{aligned} \quad (\text{A1})$$

First note that the dc level supplied to the nonlinear transducer, given by the time average of  $v(t)$ , is

$$\langle v(t) \rangle = (1/2)h_0(m^2 a_1 b_1) \cos(p) + h_0 a_2 b_2 d^2. \quad (\text{A2})$$

If this dc term were independent of modulation, then the proof would be complete: Reducing  $m$  would reduce only the range of the ac signal around a fixed dc level, and thus  $v(t)$  at small modulations would be contained within the range of  $v(t)$  at large modulations. The monotonic nonlinearity would not change this fact. However, the dc level does vary with  $m$ , so we must show that the minimum of  $v(t)$  when  $m = 1$  is lower than the minimum at  $m = 0.25$ ; i.e.,

$$\min_t [v(t)|m = 1] \leq \min_t [v(t)|m = 0.25] \quad \text{for all } p, q_1, q_2.$$

We shall demonstrate that

$$\min_t [v(t)|m = 1] \leq \min_t [v(t)|m = 0] \quad \text{for all } p, q_1, q_2.$$

Since, for any choices of  $p$ ,  $q_1$ , and  $q_2$ ,  $\min[v(t)]$  is a monotonic function of  $m$ , the second inequality (with  $m = 0$  on the right-hand side) implies the first inequality (with  $m = 0.25$  on the right-hand side). [We can ignore the behavior of the maximum of  $v(t)$ , given the results shown in Fig. 11, since the 25% data fall below the 100% data.]

Examining Eq. (A1) with  $m = 1$  and  $m = 0$ , we can see that the right-hand side of the inequality is a constant ( $h_0 a_2 b_2 d^2$ ), which also appears on the left-hand side. Subtracting this term from both sides and leaving  $m = 1$  on the left yields

$$\begin{aligned} \min_t \left[ \frac{h_0 a_1 b_1}{2} \cos(p) + \frac{h_2 a_1 b_1}{2} \cos(2ft - p - q_2) \right. \\ \left. + h_1 a_2 b_1 d \cos(ft - p - q_1) \right. \\ \left. + h_1 a_1 b_2 d \cos(ft - q_1) \right] \leq 0. \end{aligned} \quad (\text{A3})$$

To simplify inequality (A3) we combine the two 1f terms:

$$h_1 a_2 b_1 d \cos(ft - p - q_1) + h_1 a_1 b_2 d \cos(ft - q_1) \\ = A \cos(ft - Q),$$

where

$$A = h_1 d [(a_2 b_1)^2 + (a_1 b_2)^2 + 2a_1 a_2 b_1 b_2 \cos(p)]^{1/2},$$

$$Q = \arctan \frac{a_2 b_1 \sin(p + q_1) + a_1 b_2 \sin(q_1)}{a_2 b_1 \cos(p + q_1) + a_1 b_2 \cos(q_1)}.$$

We also express the  $2f$  term as a product of the two  $1f$  terms. That is,

$$\frac{h_2 a_1 b_1}{2} \cos(2ft - p - q_2) \\ = \frac{h_2 a_1 b_1}{2} \left[ 2 \cos^2 \left( ft - \frac{p + q_2}{2} \right) - 1 \right].$$

Rewriting inequality (A3), we have

$$\min_t \left[ \frac{h_0 a_1 b_1}{2} \cos(p) - \frac{h_2 a_1 b_1}{2} + h_2 a_1 b_1 \right. \\ \left. \times \cos^2 \left( ft - \frac{p + q_2}{2} \right) + A \cos(ft - Q) \right] \leq 0. \quad (\text{A4})$$

The left-hand side of inequality (A4) consists of two constants:

$$\frac{h_0 a_1 b_1}{2} \cos(p), \quad -\frac{h_2 a_1 b_1}{2},$$

and two harmonic terms:

$$h_2 a_1 b_1 \cos^2 \left( ft - \frac{p + q_2}{2} \right), \quad A \cos(ft - Q).$$

The minimum of the sum of the two harmonic terms is always negative or zero, regardless of the phase relationship or the relative amplitudes. Thus inequality (A4) is true if the sum of the two constants is less than or equal to zero. That is,

$$\frac{h_0 a_1 b_1}{2} \cos(p) - \frac{h_2 a_1 b_1}{2} \leq 0$$

or

$$h_0 \cos(p) \leq h_2. \quad (\text{A5})$$

Since  $H$  is high pass,  $h_2 \geq h_0$ , so inequality (A5) is satisfied in all cases. The nonlinearity changes the relationship between the values but does not alter their rank order. Thus no model of the form shown in Fig. 12 can account for the modulation data shown in Figs. 10 and 11, where the  $m = 25\%$  data fall below the  $m = 100\%$  data.

## ACKNOWLEDGMENTS

This research was supported by National Institutes of Health grants EYO4395, EYO9172, and EYO6629. We thank Al Eisner and Don Hood for constructive reviews.

Address all correspondence to S. Burns.

## REFERENCES AND NOTES

1. R. M. Shapley and C. Enroth-Cugell, "Visual adaptation and retinal gain controls," N. Osborne and G. Chader, eds., *Progress in Retinal Research*, 3rd ed. (1984), pp. 263–346.
2. D. C. Hood and M. A. Finkelstein, "Sensitivity to light," K. R. Boff, L. Kaufman, and J. P. Thomas, eds., *Handbook of Perception and Human Performance. Vol. 1. Sensory Processes and Perception* (Wiley, New York, 1986), pp. 5-1, 5-66.
3. N. Graham and D. C. Hood, "Modeling the dynamics of light adaptation: the merging of two traditions," *Vision Res.* **32**, 1373–1393 (1992).
4. H. deLange, "Research into the dynamic nature of the human fovea-cortex systems with intermittent and modulated light. I. Attenuation characteristics with white and colored light," *J. Opt. Soc. Am.* **48**, 777–784 (1958).
5. D. H. Kelly, "Visual responses to time-dependent stimuli. I. Amplitude sensitivity measurements," *J. Opt. Soc. Am.* **51**, 422–429 (1961).
6. G. Sperling and M. M. Sondhi, "Model for visual luminance discrimination and flicker detection," *J. Opt. Soc. Am.* **58**, 1133–1145 (1968).
7. J. A. J. Roufs, "Dynamic properties of vision. II. Theoretical relationship between flicker and flash thresholds," *Vision Res.* **12**, 279–292 (1972).
8. D. A. Baylor, A. L. Hodgkin, and T. D. Lamb, "Reconstruction of the electrical responses of turtle cones to flashes and steps of light," *J. Physiol. (London)* **242**, 759–791 (1974).
9. D. Tranchina, J. Gordon, and R. M. Shapley, "Retinal light adaptation—evidence for a feedback mechanism," *Nature* **310**, 314–316 (1984).
10. K. Purpura, D. Tranchina, E. Kaplan, and R. M. Shapley, "Light adaptation in the primate retina: analysis of changes in gain and dynamics of monkey retinal ganglion cells," *Visual Neurosci.* **4**, 75–93 (1990).
11. W. S. Geisler, "Adaptation, afterimage and cone saturation," *Vision Res.* **18**, 279–289 (1978).
12. D. C. Hood, M. A. Finkelstein, and E. Buckingham, "Psychophysical tests of models of the response function," *Vision Res.* **19**, 401–406 (1979).
13. M. M. Hayhoe, N. I. Benimoff, and D. C. Hood, "The time-course of multiplicative and subtractive adaptation processes," *Vision Res.* **27**, 1981–1996 (1987).
14. E. H. Adelson, "Saturation and adaptation of the rod system," *Vision Res.* **22**, 1299–1312 (1982).
15. M. M. Hayhoe, M. E. Levin, and R. J. Koshel, "Subtractive processes in light adaptation," *Vision Res.* **32**, 323–333 (1992).
16. P. T. Kortum and W. S. Geisler, "Adaptation mechanisms in spatial vision. II. Flash thresholds and background adaptation," *Vision Res.* **35**, 1595–1609 (1995).
17. J. G. Robson and M. K. Powers, "Dynamics of light adaptation," in *Annual Meeting*, Vol. 11 of 1988 OSA Technical Digest Series (Optical Society of America, Washington D.C., 1988), p. 67.
18. D. C. Hood, N. Graham, T. E. Wiegand, and V. M. Chase, "Probed-sinewave paradigm: a test of models of light-adaptation dynamics," *Vision Res.* **37**, 1177–1191 (1997).
19. T. E. Wiegand, D. C. Hood, and N. Graham, "Testing a computational model of light-adaptation dynamics," *Vision Res.* **35**, 3037–3051 (1995).
20. R. M. Boynton, J. F. Sturr, and M. Ikeda, "Study of flicker by increment threshold technique," *J. Opt. Soc. Am.* **51**, 196–201 (1961).
21. G. M. Shickman, "Visual masking by low-frequency sinusoidally modulated light," *J. Opt. Soc. Am.* **60**, 107–117 (1970).
22. K. Maruyama and M. Takahashi, "Wave form of flickering stimulus and visual masking function," *Tohoku Psychol. Folia* **36**, 120–133 (1977).
23. V. M. Chase, T. E. Wiegand, D. C. Hood, and N. Graham, "Exploring the dynamics of light adaptation using a sinusoidally modulated background and a probe," *Invest. Ophthalmol. Visual Sci. Suppl.* **34**, 1036 (1993).

24. S. Wu, S. A. Burns, and A. E. Elsner, "Effects of flicker adaptation and temporal gain control on the flicker ERG," *Vision Res.* **35**, 2943–2953 (1995).
25. R. M. Shapley and J. D. Victor, "The contrast gain control of the cat retina," *Vision Res.* **19**, 431–434 (1979).
26. S. A. Burns, M. R. Kreitz, and A. E. Elsner, "Computer-controlled two-color laser-based optical stimulator for vision research," *Appl. Opt.* **30**, 2063–2065 (1991).
27. S. Wu, S. A. Burns, A. Reeves, and A. E. Elsner, "Flicker brightness enhancement and visual nonlinearity," *Vision Res.* **36**, 1573–1583 (1996).
28. W. H. Swanson, T. Ueno, V. C. Smith, and J. Pokorny, "Temporal modulation sensitivity and pulse detection thresholds for chromatic and luminance perturbations," *J. Opt. Soc. Am. A* **4**, 1992–2005 (1987).
29. The conventional expression of a Gaussian-windowed sine-wave stimulus has the following form:
 
$$\exp[-(2\pi ft/2\sigma_f')^2]\sin(2\pi ft).$$
 Thus  $\sigma_f^2 = 2\sigma_f'^2$ .  
 The standard deviation of the Gaussian envelope in the time domain is
 
$$\sigma_t = \sigma_f/2\pi f = \sigma_f/\sqrt{(2)2\pi f}.$$
 With  $f = 30$  Hz and  $\sigma_f = 20$  cycles,  $\sigma_t = 20/\sqrt{(2)2\pi 30} = 75$  ms. Thus, within one  $\sigma_t$ , we can see approximately  $75/33 = 2.3$  cycles of the stimulus (Fig. 1).
30. R. A. Smith, "Adaptation of visual contrast sensitivity to specific temporal frequencies," *Vision Res.* **10**, 275–279 (1970).
31. Because of the finite duration of the test (2 ms), superimposition of it on the sinusoidally modulated background reduces the effective background modulation. We computed this modulation reduction by convolving the 2-ms pulse with a background stimulus. At 50 Hz, modulation was reduced to 98.8%, and we therefore ignored this difference.
32. This is actually an underestimation. On a 30-Hz flickering background, for example, the 2-ms test covered a phase angle of 21.6 deg. Thus, as mentioned above, the finite duration of the test introduces a certain degree of temporal smearing, resulting in an underestimate of the actual sensitivity change.
33. The phase shifts that we used in the phase adjustment were small ( $<23$  deg, for background frequencies between 20 and 40 Hz. Data at higher frequencies showed too little variation with background phase to be important to our conclusions). The purpose of the phase adjustment was to regularize only the data. The phase adjustment affects only our data presentation, not our conclusions. The change in the dc level is entirely independent of the phase adjustment.
34. G. Sperling, "Temporal and spatial visual masking. I. Masking by impulse flashes," *J. Opt. Soc. Am.* **55**, 541–559 (1965).